Profile estimation of a cable-driven continuum robot with general cable routing

Ashwin K. P.[1] and Ashitava Ghosal[1]

Dept. Mechanical Engineering, Indian Institute of Science, Bangalore, India
asitava@iisc.ac.in,
WWW home page: www.mecheng.iisc.ac.in/

Abstract. Cable-driven continuum robots find applications in bio-inspired robotics and medical robotics. Kinematics of cable-driven continuum robots, also called elephant-trunk robots, with straight cable routing is well studied in the literature. However, there are very few studies on the kinematics of continuum robots with general cable routing, despite its certain advantages. In this paper, an optimization based strategy is proposed to estimate the forward kinematics of a continuum robot with arbitrary and general cable routing. For a given displacement of the cables and cable routing, the pose of a continuum robot is obtained. Using experiments conducted on a cable driven robot, it is demonstrated that the optimization based model provides a good estimate of the forward kinematics with maximum error less than 5% of maximum tip deflection. The developed model is particularly useful since it may be possible to synthesize robots that can be deformed to desired shapes using the same theoretical framework.

Keywords: Flexible robots, Forward kinematics, General routing

1 Introduction

Continuum robots consist of a set of flexible links whose movement is character-ized by bending the links as opposed to rigid linked robots where the links are actuated at the joints. These robots deform and take shapes of smooth curves during actuation and mimic many biological systems [1]. This feature, along with the capacity to make them miniature and lightweight, has made continuum robots a topic of popular interest in robotics research (see [2] and [3]). One of the earliest continuum robots available in literature is the cable-driven elephant trunk robot (Rice/Clemson robot) shown in [4] (refer Fig. 1). The main part of the robot is a flexible *backbone* connected by a series of universal joints. On this backbone, a series of spacers is attached with equal spacing between them. The spacer consists of holes through which cables(tendons) can be routed from the base of the robot to the tip of the robot. The cables are fastened only to the topmost spacer of the robot so that when they are pulled from the base-end, the entire robot deforms and can take different shapes. An analysis of workspace of the robot can be found in [5]. A serial alignment of such robots will form a

multi-segmented continuum robot with each robot forming a segment that can be independently actuated.

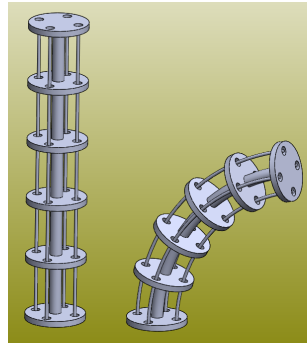Fig. 1: Elephant trunk robot [4]

Fig. 2: Elephant trunk robot configuration

In most robots, four cables are routed parallel to the backbone, with two opposing pairs of cables along the periphery of backbone, equispaced from each other (see Fig. 2). A detailed analytical expression for the kinematics of such robot is derived based on differential geometry by Gravagne and Walker [4]. The pose of actuated robot can be theoretically calculated by knowing the final lengths of the actuated cables, and this constitutes the forward kinematics of the robot. In reference [7], the authors have shown a formal proof that the forward kinematics can also be solved by posing the kinematics problem as a minimization problem, applied on a series of discretized segments of the robot – each discretised segment being a four-bar mechanism. The method is particularly interesting since it can be shown that the forward kinematics of a robot with general cable routing can also be estimated using the same optimization framework and this is the content of this paper. The advantages in using a generally routed cable driven robot can be seen from the example of helically routed robot discussed in [6]. As opposed to the mathematical framework used in [8], this approach is simpler to implement and is not restricted to routings that can be expressed analytically.

In section 2, the discretization strategy and minimization procedure is explained. Section 3 details the specifications of the robot used and the experiment set-up. The section also compares the theoretically obtained forward kinematic solutions to the experimental results which demonstrates that the theoretical model forms a good estimate for the forward kinematics. Conclusions are presented in section 4.

2   Forward kinematics of generally routed cable-driven continuum robot

For cables routed parallel to the backbone, it is theoretically proven in [4] that the shape of an actuated robot will be that of an arc of a circle. For the case of general cable routing, we use one cable (as mentioned in [8]) which is routed through holes in the spacer disks that are not aligned directly above (or below) each other so that the initial profile of the cable will not be same as that of the backbone (see Fig. 3). In this section, we discuss the discretization strategy as well as the application of minimization method to such a system.
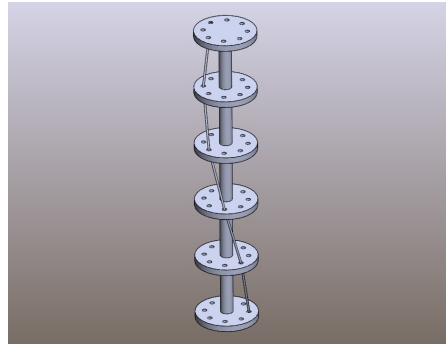

Fig. 3: Continuum robot with cable routed in an unorthodox path

In this formulation, we assume the robot as a set of serially connected four-bar linkages. Fig. 4 shows the actuated profile of a robot which has straight cable routing and five sets of four-bar linkages super-imposed on the profile. Fig. 5 shows one such linkage in the undeformed and deformed position. For one segment of the robot, the vertices of linkage are defined as follows:

1. The point where the ith spacer disk is connected to the backbone. This co-ordinate is termed $\mathbf{X}_0^i$
2. The centre of the hole in the ith spacer disk where the cable is routed. This co-ordinate is termed $\mathbf{X}_a^i$.
3. The centre of the hole in the subsequent spacer disk where the cable is routed. This co-ordinate is termed $\mathbf{X}_a^{i+1}$.
4. The point where the subsequent spacer disk is connected to the backbone. This co-ordinate is termed $\mathbf{X}_0^{i+1}$.

With reference to Fig. 5, for the four-bar linkage, the line segments a) $\overline{\mathbf{X}_0^i \ \mathbf{X}_a^i}$ forms the fixed link, b) $\overline{\mathbf{X}_a^i \ \mathbf{X}_a^{i+1}}$ forms the first crank, c) $\overline{\mathbf{X}_a^{i+1} i \ \mathbf{X}_0^{i+1}}$ forms the coupler link and d) $\overline{\mathbf{X}_0^{i+1} \ \mathbf{X}_0^i}$ forms the second crank. The distances $\|\mathbf{X}_0^i - \mathbf{X}_a^i\|$ and $\|\mathbf{X}_0^{i+1} - \mathbf{X}_a^{i+1}\|$ are fixed and are the distances between backbone and holes. Mostly, the holes for routing cables are equidistant from the backbone and hence,
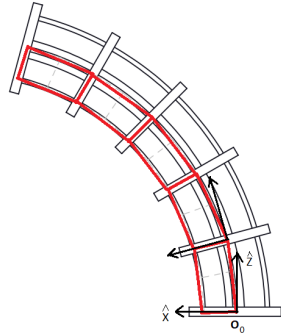
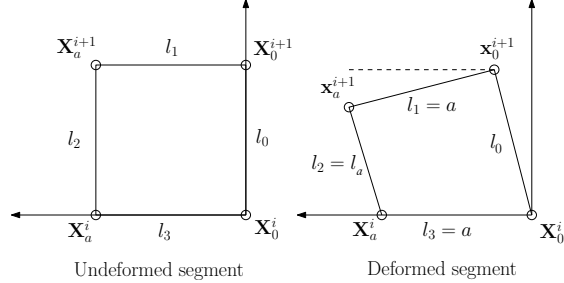Fig. 4: Discretization of robot(Red line segments show links of four-bar mechanisms)

Fig. 5: Nomenclature for four-bar linkage

$l_1 = l_3 = a$, a constant. The distance $\|\mathbf{X}_0^{i+1} - \mathbf{X}_0^i\|$ is denoted by l_0, which is the total length of backbone L_0 divided by the total number of segments n in the robot. The distance $\|\mathbf{X}_a^{i+1} - \mathbf{X}_a^i\|$ is the length of cable in each segment, $l_2 = l_a$, which could be different for each segments depending on the choice of cable routing. After actuation, the quantities $\mathbf{X}_{(\cdot)}^i$ change to $\mathbf{x}_{(\cdot)}^i$ as shown in Fig. 5.

For straight cable routing with two cables actuated together, there will be two four-bar linkages for each segment, where both the linkages share the same second crank (see Fig. 6 and Fig. 7). It has been proved in [7] that the resulting profile of the robot (backbone) upon actuation of the cables is the one which simultaneously minimizes the difference in coupler angles of the adjoined four-bar linkages from its original position. The same can be expressed mathematically as follows:
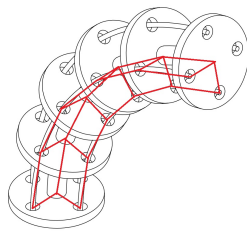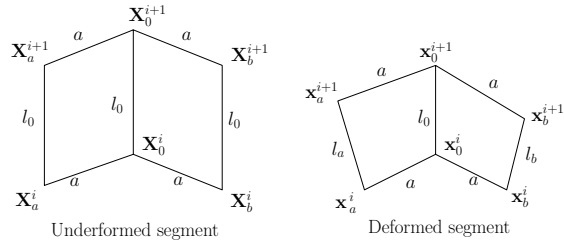

Fig. 6: Discretization of robot in 3D

Fig. 7: Nomenclature of segment in 3D

$$\underset{\mathbf{x}_b^{i+1}, \mathbf{x}_a^{i+1}, \mathbf{x}_0^{i+1}}{\arg\min} \quad \left[\arccos\left(\left(\frac{\mathbf{X}_0^i - \mathbf{X}_a^i}{\|\mathbf{X}_0^i - \mathbf{X}_a^i\|}\right) \cdot \left(\frac{\mathbf{x}_0^{i+1} - \mathbf{x}_a^{i+1}}{\|\mathbf{x}_0^{i+1} - \mathbf{x}_a^{i+1}\|}\right)\right)\right]^2 + \quad (1)$$

$$\left[\arccos\left(\left(\frac{\mathbf{X}_0^i - \mathbf{X}_b^i}{\|\mathbf{X}_0^i - \mathbf{X}_b^i\|}\right) \cdot \left(\frac{\mathbf{x}_0^{i+1} - \mathbf{x}_b^{i+1}}{\|\mathbf{x}_0^{i+1} - \mathbf{x}_b^{i+1}\|}\right)\right)\right]^2$$

Subject to:

$$\|\mathbf{x}_0^{i+1} - \mathbf{X}_0^i\| = l_0 \qquad\qquad (2)$$
$$\|\mathbf{x}_a^{i+1} - \mathbf{X}_a^i\| = l_a$$
$$\|\mathbf{x}_b^{i+1} - \mathbf{X}_b^i\| = l_b$$
$$\|\mathbf{x}_0^{i+1} - \mathbf{x}_a^{i+1}\| = a$$
$$\|\mathbf{x}_0^{i+1} - \mathbf{x}_b^{i+1}\| = a$$
$$\arccos\left(\left(\frac{\mathbf{x}_0^i - \mathbf{x}_a^i}{\|\mathbf{x}_0^i - \mathbf{x}_a^i\|}\right) \cdot \left(\frac{\mathbf{x}_0^i - \mathbf{x}_b^i}{\|\mathbf{x}_0^i - \mathbf{x}_b^i\|}\right)\right) - \arccos\left(\left(\frac{\mathbf{X}_0^i - \mathbf{X}_a^i}{\|\mathbf{X}_0^i - \mathbf{X}_a^i\|}\right) \cdot \left(\frac{\mathbf{X}_0^i - \mathbf{X}_b^i}{\|\mathbf{X}_0^i - \mathbf{X}_b^i\|}\right)\right) = 0$$

Given data: $\mathbf{X}_0^i, \mathbf{X}_0^{i+1}, \mathbf{X}_a^i, \mathbf{X}_a^{i+1}, \mathbf{X}_b^i, \mathbf{X}_b^{i+1}, l_0, l_a, l_b, a$

where the subscript 'b' represents the quantities for the second four-bar linkage.

The first five equality constraints ensures that the given dimensions are maintained, while the last constraint ensures that the space between the cables is maintained on the spacer disk. The solution procedure consists of solving the pose of the base segment and progressively moving till the free end of the robot. The resulting profile of the robot is a curve in 3D space.

For the case where single cable is routed through a non-linear path, a 3D profile is obtained without the use of an additional cable. This is because now the four-bar linkage in a discretized segment is not a planar mechanism unlike in a straight routed case. Hence, we assume the adjoining linkage b from the above formulation as a virtual linkage shown in Fig. 8. With reference to equation (1), we assume that the 3-dimensional deformation of robot is characterized by the minimization of coupler angles of those couplers which are mutually perpendicular to each other–as is the case for straightly-routed robots. Taking this reasoning into account, we modify the above equations as follows:

$$\underset{\mathbf{x}_0^{i+1}, \mathbf{x}_a^{i+1}}{\arg\min} \quad \left[\arccos\left(\left(\frac{\mathbf{X}_0^i - \mathbf{X}_a^i}{\|\mathbf{X}_0^i - \mathbf{X}_a^i\|}\right) \cdot \left(\frac{\mathbf{x}_0^{i+1} - \mathbf{x}_a^{i+1}}{\|\mathbf{x}_0^{i+1} - \mathbf{x}_a^{i+1}\|}\right)\right)\right]^2 + \quad (3)$$

$$\left[\arccos\left(\left(\frac{\mathbf{X}_0^i - \bar{\mathbf{X}}_b^i}{\|\mathbf{X}_0^i - \bar{\mathbf{X}}_b^i\|}\right) \cdot \left(\frac{\mathbf{x}_0^{i+1} - \mathbf{x}_b^{i+1}}{\|\mathbf{x}_0^{i+1} - \mathbf{x}_b^{i+1}\|}\right)\right)\right]^2$$

Subject to:

$$\|\mathbf{x}_0^{i+1} - \mathbf{X}_0^i\| = l_0 \qquad\qquad (4)$$
$$\|\mathbf{x}_a^{i+1} - \mathbf{X}_a^i\| = l_a$$
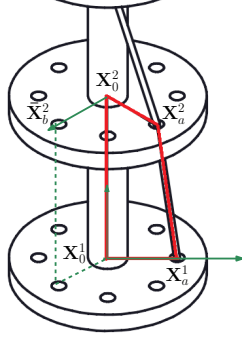$$\|\mathbf{x}_0^{i+1} - \mathbf{x}_a^{i+1}\| = a$$

Fig. 8: Discretization of generally routed robot(Four-bar linkage shown in red)
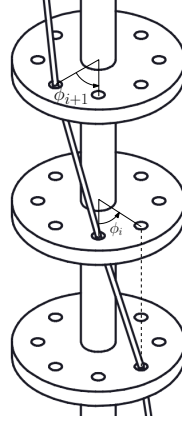

Fig. 9: Cable progresses at ϕ_i angles

Given data: $\mathbf{X}_0^i, \mathbf{X}_0^{i+1}, \mathbf{X}_a^i, \mathbf{X}_a^{i+1}, l_0, l_a, a$

where the co-ordinate $\mathbf{X}_b^{i+1}$ is chosen to be that point in the spacer disk which is perpendicular to the coupler link $\overline{\mathbf{X}_a^{i+1}\mathbf{X}_0^{i+1}}$,

$$\bar{\mathbf{X}}_b^i = a \frac{\left(\mathbf{X}_a^i - \mathbf{X}_0^i\right) \times \left(\mathbf{X}_0^{i+1} - \mathbf{X}_0^i\right)}{\| \left(\mathbf{X}_a^i - \mathbf{X}_0^i\right) \times \left(\mathbf{X}_0^{i+1} - \mathbf{X}_0^i\right) \|} \tag{5}$$

It may be noted that the same formulation is valid for a robot with linear routing as well.

The algorithm to obtain the profile of the cable and the backbone is as follows:

1. A co-ordinate system $\mathcal{O}_0$ is defined at the centre of the base of the robot with origin as the centre of the first(base) spacer disk. Z-axis is chosen along the axis of the robot. X-axis in the direction of the hole in the base disk where the cable is routed and a Y-axis is that which forms a right-handed co-ordinate system.

2. Solve the equation (3) for the ith segment ($i = 1$ for the first segment) and obtain the values of $\mathbf{x}_a^{i+1}$ and $\mathbf{x}_0^{i+1}$

3. Find $\hat{i} = \dfrac{\mathbf{x}_a^{i+1} - \mathbf{x}_0^{i+1}}{\|\mathbf{x}_a^{i+1} - \mathbf{x}_0^{i+1}\|}$, $\quad \hat{k} = \dfrac{\mathbf{x}_0^{i+1} - \mathbf{X}_0^i}{\|\mathbf{x}_0^{i+1} - \mathbf{X}_0^i\|}$, $\quad \hat{j} = \hat{k} \times \hat{i}$ and the transformation to the co-ordinate system $\mathcal{O}_i$ using the matrix
$\mathbf{T} = \begin{bmatrix} \hat{i} \ \hat{j} \ \hat{k} \ \mathbf{x}_0^{i+1} \\ 0 \ 0 \ 0 \quad 1 \end{bmatrix}$

4. Assign $\mathbf{x}_0^{i+1} \to \mathbf{X}_0^i, \mathbf{x}_a^{i+1} \to \mathbf{X}_a^i, \left[\left(\mathbf{X}_0^{i+1}\right)^T, 1\right]^T = \mathbf{T}\left[0, 0, l_0, 1\right]^T$ and
$\left[\left(\mathbf{X}_a^{i+1}\right)^T, 1\right]^T = \mathbf{T}\left[a\cos\phi_i, a\sin\phi_i, l_0, 1\right]^T$, where ϕ_i is the angle at which the cable is progressed in each segment (see Fig. 9).

5. Repeat steps 2 to 4 till $i = 1, 2, \ldots, n$

In the following section, we present numerical and experimental results with prototype robots which show that the above numerical solutions are a good estimate for the profile of a physically actuated continuum robot.

3 Numerical and experimental results

Unlike the theory for straight cable routing, there has not been many studies regarding the kinematics of robot with general cable routing. In [8], the authors used Cosserat rod theory and solved the statics of a generally routed cable driven robot. Since their procedure is intended mainly to study the statics of the robot, the formulation depends heavily on the material properties of the constituent components as well as the applied forces. Due to the unavailability of a kinematics formulation for generally routed robot, a formal comparison is not possible at present and, in this paper, we compare the theoretical results with the results obtained from experiments conducted on a robot prototype.

To this end, we used a 3D printed robot prototype made of Verowhite resin. The robot is 182 mm long with 10 spacer disks of 2 mm each attached at equal spacing on a backbone of diameter 1.5 mm. This fixes the length l_0 as 20 mm. The disks have 12 holes of 1.3 mm diameter arranged in a the periphery of a circle with 8 mm radius. Hence, we have $a = 8$ mm for this robot. For the cable, we used nylon cords of diameter 0.5 mm and is attached to the topmost spacer. The deformation of the robot is captured using a camera, and the profile obtained from theoretical formulation is super-imposed on the images for comparison. For all the experiments, we pull the cable by a certain amount, and assume that the reduction of lengths of each cable segment is proportional. i.e., if the cable is pulled by δ mm, we assume that the length l_a^i for the ith segment changes as $l_a^i \to l_a^i \left(1 - \dfrac{\delta}{L_a} \right)$ where L_a is the initial length of the cable in the robot.

The optimization problem was solved using `fmincon` routine in MATLAB® and takes about 15 seconds in an Intel processor at 2.00 GHz and 8 GB RAM. For validation, we used three cable routings: a) $\phi_i = 30°, i = 1, 2, \ldots, n$, b) $\phi_i = 60°, i = 1, 2, \ldots, n$ and $\phi = \{30°, 30°, 30°, 30°, 0°, -30°, -30°, -30°, -30°\}$. Figures 10, 11 and 12 show the initial configurations as well as the profiles after actuation of the robot. The green markers in the figures point to the co-ordinates $\mathbf{x}_0$ and the red markers depict $\mathbf{x}_a$ where $\mathbf{x}_0$ and $\mathbf{x}_a$ denote the co-ordinates of the points on the backbone and the cables, respectively. The cable profile (dark solid line), the backbone and the disks for the three cases are also shown in figures 10, 11 and 12. It can be seen that the numerically computed points (green and red markers) are very close to the experimental results obtained with the hardware.

It may be noted that the theoretical formulation is subject to errors due to factors such as:

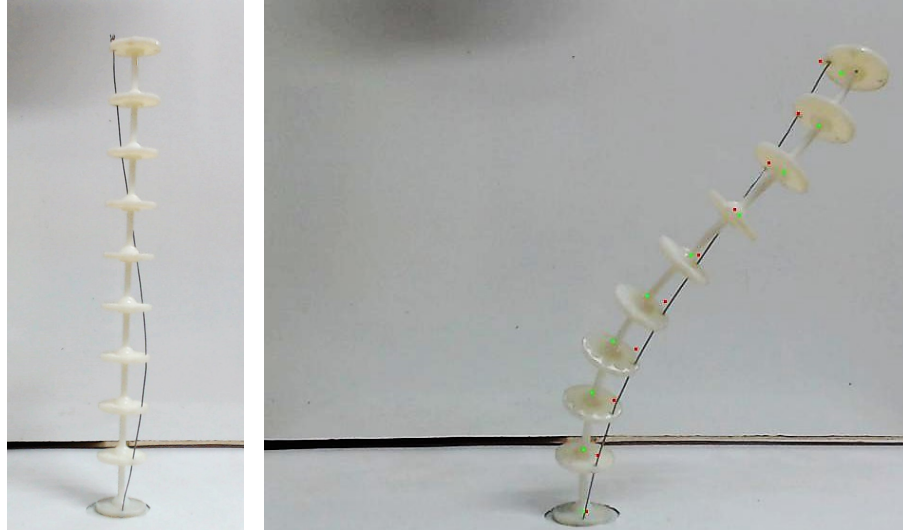1. Assumption that the lengths of cable are proportionally scaled during actuation,

Fig. 10: Initial and actuated configurations of a continuum robot with $\phi_i = 30°, i = 1, 2, .., 9$

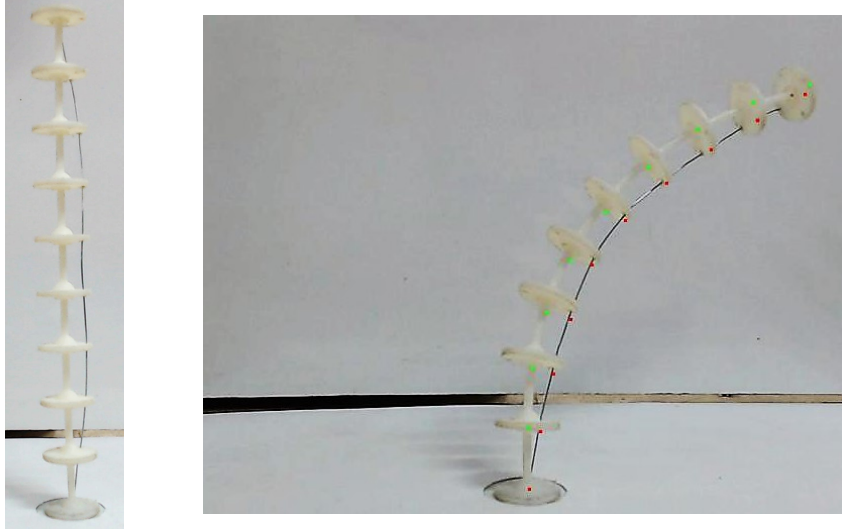Fig. 11: Initial and actuated configurations of a continuum robot with $\phi_i = 60°, i = 1, 2, .., 9$

Fig. 12: Initial and actuated configurations of a continuum robot with $\phi = \{30°, 30°, 30°, 30°, 0°, -30°, -30°, -30°, -30°\}$

2. Bending/deflection of backbone, and
3. Clearance between the cable and the walls of hole.

We can see that in spite of these errors, the optimization based approach gives a very good estimate of the profile of the actuated robot with a maximum error of 4 mm in all cases – this is less than 5% of maximum deflection at the tip.

4   Conclusions

In this paper, we have demonstrated that the profile of a cable-driven continuum robot with the cable routed in a general, not necessarily straight, path can be estimated using an optimization based method. In this method, the robot is first assumed to be a series of connected four-bar linkages, and the pose of a segment of the actuated robot is assumed to be the final configuration of the four-bar mechanism. The key idea is that minimization of the change of angle made by the coupler link from its initial value gives the pose of actuated segment. By iteratively proceeding from the base segment to the segment at the tip of the robot, the complete profile is obtained. From experiments conducted on a continuum robot with flexible backbone and equally spaced disks, it is shown that the proposed method gives a good estimate of the forward kinematics of a generally-routed cable driven continuum robot.

From the formulation, we can see that the inverse kinematics problem– finding the route of the cable given a desired final profile – may be achieved from the

same formulation only by changing the optimization variables. The inverse problem will be particularly interesting since it may help to synthesize mechanisms capable of deforming to a desired shape. This work is continuing.

References

1. Kim, S., Laschi, C., Trimmer, B. : Soft robotics: a bioinspired evolution in robotics. Trends. Biotechnol. 31(5), 287-294(2013). doi.org/10.1016/j.tibtech.2013.03.002
2. Walker, I.D., : Continuous backbone continuum robot manipulators. ISRN. Rob. 726506 (2013). doi.org/10.5402/2013/726506
3. Burgner-Kahrs, J., Rucker, D.C. and Choset, H. : Continuum robots for medical applications: A survey. IEEE. TRO. 31(6), 1261-1280 (2015). doi:10.1109/TRO. 2015.2489500
4. Gravagne, I.A., Walker, I.D. : On the kinematics of remotely-actuated continuum robots. In: IEEE International Conference on Robotics and Automation, pp. 2544-2550. IEEE, (2000). doi:doi.org/10.1002/rob.10070
5. Cao, K., Kang, R., Wang, J., Song, Z., Dai, J. : Kinematic model and workspace analysis of tendon-driven continuum robots. In: Proceedings of the 14th IFToMM World Congress, pp. 640-644. Taipei, Taiwan (2015).
6. Starke, J., Amanov, E., Chikhaoui, M.T., Burgner-Kahrs, J.,: On the merits of helical tendon routing in continuum robots. In: IEEE/RSJ International Conference on Intelligent Robots and Systems(IROS), pp. 6470-6476. IEEE, (2017). doi:10. 1109/IROS.2017.8206554
7. Ashwin, K. P., Ghosal, A.: Forward kinematics of cable-driven continuum robot using optimization method. In: Proceedings of 5th Asian Conference on Mechanisms and Machine Science, December 17-20, 2018.
8. Rucker, D.C., Webster III, R.J. : Statics and dynamics of continuum robots with general tendon routing and external loading. IEEE. TRO. 27(6), 1033-1044 (2011). doi:10.1109/TRO.2011.2160469